



**HAL**  
open science

## The application of TMAH thermochemolysis on the detection of nucleosides: applications for the SAM and MOMA instruments

Yuanyuan He, Arnaud Buch, Cyril Szopa, Amy Williams, Caroline Freissinet, Melissa Guzman, Maeva Millan, David Coscia, Jean-Yves Bonnet, Michel Cabane

### ► To cite this version:

Yuanyuan He, Arnaud Buch, Cyril Szopa, Amy Williams, Caroline Freissinet, et al.. The application of TMAH thermochemolysis on the detection of nucleosides: applications for the SAM and MOMA instruments. *Journal of Analytical and Applied Pyrolysis*, 2022, 168 (November), pp.105790. 10.1016/j.jaap.2022.105790 . insu-03859873

**HAL Id: insu-03859873**

**<https://insu.hal.science/insu-03859873v1>**

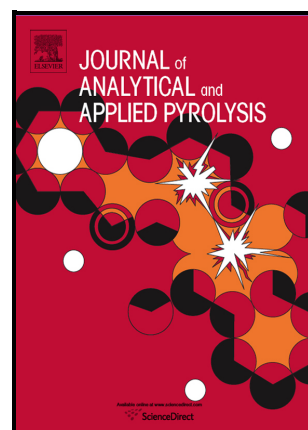
Submitted on 18 Nov 2022

**HAL** is a multi-disciplinary open access archive for the deposit and dissemination of scientific research documents, whether they are published or not. The documents may come from teaching and research institutions in France or abroad, or from public or private research centers.

L'archive ouverte pluridisciplinaire **HAL**, est destinée au dépôt et à la diffusion de documents scientifiques de niveau recherche, publiés ou non, émanant des établissements d'enseignement et de recherche français ou étrangers, des laboratoires publics ou privés.

The application of TMAH thermochemolysis on the detection of nucleosides: applications for the SAM and MOMA instruments

Yuanyuan He, Arnaud Buch, Cyril Szopa, Amy Williams, Caroline Freissinet, Melissa Guzman, Maëva Millan, David Coscia, Jean-Yves Bonnet, Michel Cabane



PII: S0165-2370(22)00360-6

DOI: <https://doi.org/10.1016/j.jaap.2022.105790>

Reference: JAAP105790

To appear in: *Journal of Analytical and Applied Pyrolysis*

Received date: 7 July 2022

Revised date: 29 October 2022

Accepted date: 11 November 2022

Please cite this article as: Yuanyuan He, Arnaud Buch, Cyril Szopa, Amy Williams, Caroline Freissinet, Melissa Guzman, Maëva Millan, David Coscia, Jean-Yves Bonnet and Michel Cabane, The application of TMAH thermochemolysis on the detection of nucleosides: applications for the SAM and MOMA instruments, *Journal of Analytical and Applied Pyrolysis*, (2022) doi:<https://doi.org/10.1016/j.jaap.2022.105790>

This is a PDF file of an article that has undergone enhancements after acceptance, such as the addition of a cover page and metadata, and formatting for readability, but it is not yet the definitive version of record. This version will undergo additional copyediting, typesetting and review before it is published in its final form, but we are providing this version to give early visibility of the article. Please note that, during the production process, errors may be discovered which could affect the content, and all legal disclaimers that apply to the journal pertain.

## **The application of TMAH thermochemolysis on the detection of nucleosides: applications for the SAM and MOMA instruments**

Yuanyuan He<sup>1\*</sup>, Arnaud Buch<sup>1</sup>, Cyril Szopa<sup>2</sup>, Amy Williams<sup>3,4</sup>, Caroline Freissinet<sup>2</sup>, Melissa Guzman<sup>2</sup>, Maëva Millan<sup>4,5</sup>, David Coscia<sup>2</sup>, Jean-Yves Bonnet<sup>4,7</sup>, Michel Cabane<sup>2</sup>

<sup>1</sup> Laboratoire Génie des Procédés et Matériaux, CentraleSupélec, University Paris-Saclay, 8-10 rue Joliot-Curie, 91190, Gif-sur-Yvette, France.

<sup>2</sup> LATMOS/IPSL, UVSQ Université Paris-Saclay, Sorbonne Université, CNRS, 11 Bd d'Alembert, 78280 Guyancourt, France.

<sup>3</sup> Space Science Exploration Division (Code 690), NASA Goddard Space Flight Center, Greenbelt, Maryland, USA.

<sup>4</sup> Department of Geological Sciences, University of Florida, Gainesville, FL, USA

<sup>5</sup> Georgetown University, Washington D.C., USA.

<sup>7</sup> Telespazio France, Toulouse, France

### **Abstract**

Tetramethylammonium hydroxide (TMAH) thermochemolysis has been utilized by the Curiosity rover's Sample Analysis at Mars (SAM) instrument and will be utilized by the ExoMars 2022's Mars Organic Analyzer (MOMA) instrument. TMAH thermochemolysis is one of the main techniques that enables the detection of bioindicators when it is combined with pyrolysis-gas chromatography and mass spectrometry (Py-GC/MS) at the surface of Mars. This study identifies the thermochemolysis products of targeted nucleosides using flash pyrolysis and a SAM-like ramp pyrolysis. Results indicate that the methylated nucleosides can be detected when nucleosides are submitted to TMAH thermochemolysis, which demonstrates that the TMAH thermochemolysis protocol does not result in the decomposition of the nucleosides. To detect the whole structure of each nucleoside, low thermochemolysis temperature is required. 200 °C is the optimal temperature. Methylated nucleobases are the main products of the tested nucleosides when the thermochemolysis temperature is higher than 300 °C. Furfuryl methyl ether, one of the degradation products of these nucleosides, were also identified from 200 to 600 °C in this study. These experiments will establish a reference database for interpretation of the data acquired by the SAM and MOMA experiments during operations on Mars.

### **Keywords:**

Nucleosides, TMAH thermochemolysis, Py-GC/MS, Mars, SAM

---

\* Author to whom correspondence should be addressed: E-mail address: yuanyuanhe@hotmail.com

## 1. Introduction

The Sample Analysis on Mars (SAM) instrument is one of ten instruments on the Curiosity rover designed to assess habitability on Mars and search for organic and inorganic molecules. The Mars Organic Molecule Analyzer (MOMA) instrument onboard the ExoMars 2022 rover has a main goal of looking for biochemical precursors at the Mars surface. Some known chemical biosignatures and bioindicator could be organic compounds such as fatty acids [1], amino acids and carboxylic acids [2], pigments [3], nucleobases [3], sugars/polysaccharides [3], isoprenoids, and steriods [4], etc. Among these chemical products, nucleosides, nucleotides, and nucleobases are essential components of life on Earth. They constitute essential building blocks of nucleic acids, ribonucleic acid (RNA) and deoxyribonucleic acid (DNA), and are involved in the regulation and modulation of various physiological process in the human body [5,6]. DNA, as an information carrier, stores an organism's genetic information with unique orders of four nucleobases (A, T, C, G). This method storing genetic information has proved robust across billion-year long timescales on Earth. Some studies have suggested that DNA could be placed in extremely cold regions on Earth or even on Mars to enable millennium-long preservation [7]. The first life on Earth likely used RNA, which is made up of sequences of four different nucleotides, the latter of which can be formed through a chemical reaction source. RNA polymers may have emerged very quickly after the deposition of meteorites containing nucleobases (less than a few years), and the synthesis of nucleotides and their polymerization into RNA may occur over one to a few wet-dry cycles of warm little ponds [8]. However, biological RNA and DNA are universal, unique, and very conservative. The role of RNA in the origin of life is well established, and how RNA emerged on the early Earth is one of the first steps in understanding the origin of life [9]. This means that the emergence of nucleic acids is central to many theories for the origins of life, and that opens questions including the original source and structure of the building blocks of these molecules, such as nucleobases, sugars, nucleosides and nucleotides [10]. Therefore, the formation and detection of nucleosides and nucleotide abiogenesis has been widely studied [8,11,12].

The structure of nucleobases, nucleosides, and nucleotides are well known today. Polynucleotides are composed of pentose sugar moieties linked by 3',5'-phosphodiester bonds forming a sugar-phosphate backbone [13–16]. Nucleosides such as uridine, cytidine, adenosine and thymidine can be synthesized by simple two molecule reactions, i.e., from the reaction of ribose or 2'-deoxyribose with the canonical nucleobases (cytosine, uracil, adenine, guanine, and thymine) [17]. The study of the formation of nucleosides from a one-pot reaction

makes it possible to analyze the factors that might have played a role in the condensation of nucleotides into polymers, and which led to the evolution of extant nucleic acids [18]. Abiotic phosphorylation of nucleosides is a key chemical step that may have provided nucleotides to the prebiotic world. Some minerals played a key role in that process. Borate can work in formamide to guide the reactivity of nucleosides under conditions where they are phosphorylated [19]. Adsorptions of K and Mg by goethite could also have played an important role in peptide synthesis and the formation of nucleosides [20,21]. Additionally, clays such as montmorillonite appear to play a protective role for nucleosides against ionizing radiation [22]. The survival of nucleosides exposed to a high radiation field in an aqueous solution and adsorbed on Na-montmorillonite indicates that the pyrimidine nucleosides were more resistant to heat and less resistant against ionizing radiation even when adsorbed in clay [22]. The purine-based nucleosides (adenosine and guanosine) showed a much higher radiolysis resistance than the pyrimidine-based nucleosides (cytidine and uridine) [23]. Given these results, it is perhaps unsurprising that purine nucleobases are found in practically all carbonaceous chondrite meteorites while the pyrimidine nucleobases are absent or below the detection limits of current analytical techniques [23].

Nucleobases have been found in meteorites (guanine, adenine, and uracil) with concentrations of 0.25 to 515 ppb [24,25]. Derivatives of nucleobases (guanine> hypoxanthine) have also been identified in meteorites [24,26]. In addition, purine nucleobases such as guanine and xanthine, and pyrimidine nucleobases such as cytosine, uracil and thymine have been detected in numerous meteorites previously, and the isotopic composition of nucleobases isolated from carbonaceous chondrites support their extraterrestrial origin [26–28]. In addition, sugar phosphates are the backbone of the genetic molecules DNA and RNA. Ribose is particularly essential as a building block of RNA, because it could have both stored information and catalyzed reactions in primitive life on Earth. Extraterrestrial sugars in the NWA 801 and Murchison meteorites are isotopically distinct from terrestrial sugars and provide clear evidence of an extraterrestrial origin for these sugars in primitive meteorites [29]. The structure of nucleobases and nucleosides also influence their behavior. The perpendicular structure of nucleosides makes it difficult for the nucleoside to interact with the mineral structure and consequently, nucleosides have lower adsorption than corresponding nucleobases [30]. This demonstrated that the ribose structure of nucleosides also played an important role compared to nucleobases. Above all, with the detection of extraterrestrial nucleobases and ribose (the main fragments of nucleosides), nucleosides are interesting target compounds for astrobiology even if there is less information about extraterrestrial nucleosides.

Since TMAH thermochemolysis will be applied to search for organic compounds on Mars, this study focuses on the analysis of nucleosides by TMAH thermochemolysis. Therefore, in this study, the application of TMAH thermochemolysis on six deoxynucleosides standards and mixtures pyrolyzed at different temperatures was studied. The temperature of the TMAH thermochemolysis reaction was optimized from 200 to 600°C for this set of nucleosides and all the products of these nucleosides following TMAH thermochemolysis were identified. Moreover, thermochemolysis of these nucleosides was also studied using a “slow” pyrolysis ramp ( $35\text{ }^{\circ}\text{C}\cdot\text{min}^{-1}$ ) mimicking the pyrolytic conditions of the SAM experiment in order to assess its capability to detect nucleosides. From our knowledge, this is the first study of the behavior of nucleosides submitted to TMAH thermochemolysis under a SAM-like ramp pyrolysis (from 50 to 850 °C at a heating rate of  $35\text{ }^{\circ}\text{C}\cdot\text{min}^{-1}$ ) [31]. Additionally, the thermochemolysis mechanisms of all nucleosides with TMAH were analyzed. This study provides important reference data that constrains the nucleosides or nucleoside derivatives that will be detectable using *in-situ* TMAH thermochemolysis as part of *in situ* analyses performed on Mars by the SAM and MOMA space experiments.

## 2. Experimental

### 2.1 Materials

In this study, nucleosides include deoxyadenosine (dA, Sigma,  $\geq 99\%$ , stored 2-8 °C), deoxyguanosine (dG, Sigma, 98-100%), thymidine (dT, Sigma,  $\geq 99\%$ ), 2'-deoxyuridine (dU, Sigma, 99-100%), 2'-deoxycytidine (dC, Sigma,  $\geq 99\%$ , HPLC, stored -20 °C); deoxyinosine (dI, Sigma,  $\geq 98\%$ , stored -20 °C) were used. The structures of the selected nucleosides can be seen in Figure 1. All nucleosides were dissolved in deionized water. The concentration of each nucleoside and the concentration of their mixtures are shown in Table 1. 3  $\mu\text{l}$  of TMAH (25 wt. % in methanol, Sigma) was applied in this study, which is always in excess volume and the amount of methyl functional group compared to the nucleosides. 0.2  $\mu\text{l}$  of Naphthalene-D8 at a concentration of  $0.005\text{ mol}\cdot\text{L}^{-1}$  (Sigma-Aldrich, isotopic purity, 99 atom % D) was used as the internal standard (IS).

### 2.2 Py-GC/MS and methods

The pyrolysis experiments were performed with an evolved gas analysis (EGA)/PY-3030D micro-oven pyrolyzer (Frontier Lab) installed on a Split/Splitless (SSL) injector of a Trace GC Ultra gas chromatograph (ThermoScientific) coupled to a quadrupole mass spectrometer (ISQ LT, Thermo Scientific). Flash pyrolysis and SAM-like ramp pyrolysis were applied for the tests described in this article. For the flash pyrolysis, the pyrolysis temperatures were at 200, 300, 400, 500, and 600 °C. The nucleosides solution (in H<sub>2</sub>O, 0.5 µl of dA, dT, dU, dC, dI; 1 µl of dG, respectively) was put in a small stainless-steel cup (Frontier large volume cup), followed by the addition of 3 µl of TMAH over the nucleosides solution. Then the stainless-steel cup containing a mixture of nucleosides and TMAH was quickly introduced into the oven already heated at the designated temperature. Helium (99.9999%) was used as the carrier gas to carry the volatile products from the pyrolyzer to the GC/MS. The SAM-like ramp pyrolysis is the same as in previous work [32,33]. In this process, a cup containing the sample was heated using heart-cut EGA temperature zones from 50 °C to reach the final temperature (850 °C held for 1 min) at the SAM heating rate of 35 °C·min<sup>-1</sup>. The pyrolysis sequence being too long to proceed to a sharp injection of the analytes into the GC, liquid nitrogen was used to cool down the chromatographic column inlet where the volatiles produced by the samples condense and were trapped in a small volume. Once the pyrolysis achieved, the cryogenic cooling was stopped and all the products were then released and sent to the GC/MS via the helium flow. All experiments were repeated at least 5 times each.

The GC was equipped with a Supelco SLB-5MS Inferno column (30 m × 0.25 mm i.d. × 0.25 µm film thickness). The temperature programming of the column starts at 40 °C and is held for 2 min, then ramped at a heating rate of 6 °C·min<sup>-1</sup> up to 130 °C and then heated again to 300 °C at a rate of 10 °C·min<sup>-1</sup> and maintained for 1 min. Helium was used as the carrier gas and the helium flow rate in the column was 1.2 mL·min<sup>-1</sup>. The split flow was 24 mL·min<sup>-1</sup>. The temperature of the SSL injector was set at 280 °C. The ions were scanned between *m/z* 40 and *m/z* 500. The ionization energy of the electron ionization source was 70 eV.

### 3. Results

#### 3.1 TMAH thermochemolysis for nucleosides

To determine the main reaction products of nucleosides with TMAH thermochemolysis, each nucleoside was submitted to flash pyrolysis conditions at 200 °C in the presence of TMAH. Figure 2 shows the chromatogram with the TMAH thermochemolysis

products of nucleosides following a flash pyrolysis at 200 °C. We observe that the main thermochemolysis products are the methylated dA, dT, dU, and dC for all the nucleosides analyzed except for dG and dI. Though there are various methylated compounds of nucleobases as identified in our previous study [34], the methylated compounds with the highest intensity were selected as the possible target compounds that could allow the identification of nucleosides analyzed with TMAH thermochemolysis. Table 2 shows the main products of nucleosides reaction with TMAH thermochemolysis following flash pyrolysis at 200 °C.

Following the thermochemolysis of dI at 200 °C, 1,7-dimethyl-hypoxanthine is the main byproduct with a retention time of 27.6 min. Under the same experimental condition, N, N, N'-trimethyl-cytosine is the main methylated compound produced from the dC thermochemolysis with a retention time of 27.4 min. 1,3-dimethyl-uracil is the main methylated compounds of dU with a retention time of 20.2 min. 1,3-dimethyl-thymine is the key product of dT with a retention time of 21.2 min. Isomers of tetramethyl-guanine are the main methylated products of dG following TMAH thermochemolysis and have retention times of 28.1 and 29.4 min, respectively. The production of isomers is due to the molecular structure of guanine which enables different possibilities for the replacement of polar labile hydrogens with methyl functional groups from TMAH, leading to the appearance of several peaks of methylated guanine [34]. N, N, 9-trimethyl-adenine or its isomer, N, N, 3-trimethyl-adenine, at retention times of 25.5 min and 26.8 min, respectively, are the main methylated products of dA with TMAH thermochemolysis. In addition, not only were methylated nucleobase derivatives from each nucleoside detected, but the characteristic peak of methylated ribose from the nucleoside structure was also identified at a retention time of 6.1 min. This compound was identified as 2-methoxymethyl-furan or furfuryl methyl ether and is the methylated product of ribose from the nucleoside molecule. In addition to thermal degradation products, the methylated nucleosides were also detected in our study, such as methylated dC at a retention time of 34.4 min, methylated dU (2'-deoxy-3-methyl-3,5'-di-O-methyl-uridine) at a retention time of 30.1 min, methylated dT (2'-deoxy-N,N,O-trimethyl-thymidine) at a retention time of 30.5 min, and methylated dA (2'-deoxy-N,N,O,O-tetramethyl-adenosine) at a retention time of 33.1 min. The peak intensities of the methylated nucleosides are high, which demonstrates that methylated nucleosides are thermally stable at 200°C and could be the direct evidence of the presence of DNA molecule fragments. Figure 3 shows the mass spectrum of different methylated products from nucleosides following thermochemolysis with TMAH.



In addition to the main methylated products of nucleosides with TMAH thermochemolysis, some byproducts of nucleobases are also identified following TMAH thermochemolysis at a flash pyrolysis of 200 °C, details of which can be found in Table S1-6 in the appendix.

### 3.2 Optimal temperature of nucleosides with TMAH thermochemolysis.

To determine the optimal temperature for TMAH thermochemolysis of nucleosides, we performed thermochemolysis at different temperatures from 200 °C to 600 °C. Figure 4 shows the chromatograms of the compounds produced by TMAH thermochemolysis of each nucleoside at different temperatures. For a given nucleoside, the chromatograms obtained for the different thermochemolysis temperatures are quite comparable and the compounds detected are the same. However, the peak intensities of some main products varied with temperature. For example, the abundance of 2'-deoxy-N,N,O,O-tetramethyl-adenosine (RT = 33.1 min) decreased significantly with increasing thermochemolysis temperature. And in a more general way, intense peaks observed at high retention times at 200 °C tend to decrease in intensity whereas less retained species show higher intensities. This is often representative of an increase of the fragmentation of heavy species into smaller during the TMAH thermochemolysis reaction which is allowed at higher temperatures.

Figure 5 shows the distribution of the products detected after TMAH thermochemolysis of nucleosides at different temperatures. The target peak intensity of each methylated nucleoside with TMAH thermochemolysis is the highest after flash pyrolysis at 200 °C. For dA, dT, and dU, their methylated compounds were detected, as 2'-deoxy-N,N,O,O-tetramethyl-adenosine, 2'-deoxy-N,O,O-trimethyl-thymine, 2'-deoxy-3-methyl-3',5'-di-O-methyl-uridine, respectively. With increasing temperature, the abundances of methylated nucleosides decreased, while the abundances of methylated nucleobases increased. This demonstrated that the bond between the ribose and the nucleobase is more easily broken at high temperature. Thus, the yield of methylated nucleobases increased when the temperature increased from 300 to 600 °C. For instance, the intensity of N,N,9-trimethyl-adenine at 600 °C is 2 times of that of 300 °C. Similarly, the yield of methylated ribose, 2-methoxymethyl-furan, increased with the temperature increase, which also demonstrated that the high temperatures are more favorable to break the nucleosides into their respective the nucleobases and ribose. The methylated nucleobases from the nucleosides with TMAH thermochemolysis were detected at the highest tested temperature of 600 °C. Concerning the

direct detection of nucleosides under their TMAH methylated form, it can be concluding that 200 °C is the optimal temperature because the nucleosides thermal degradation is limited at this temperature. On the other hand, the highest  $A_i/A_{is}$  value at 200 °C is very high maybe due to the lower temperature compared to the boiling temperature (218 °C) of the internal standard. However, the case may be different for nucleosides inside a solid matrix, where a higher temperature may be necessary to desorb the nucleotides from its inorganic matrix.

### 3.3 Analysis of a mixture of nucleosides

The methylated products of nucleosides and their target compounds at different temperatures have been analyzed. To determine whether there are coelutions among these nucleoside products, a mixture of the nucleosides, including dA, dU, dC, dT, and dI, has been analyzed by TMAH thermochemolysis between the temperatures of 200 to 600 °C (Figure 6). dG was not mixed with the other five nucleosides, because according to our previous research, we found that dG can decompose into caffeine, which is one of the byproducts of hypoxanthine with TMAH thermochemolysis [34]. The target peak of each nucleoside has been identified in the chromatogram. For example, the methylated compounds of dU and dT were separated completely, even if their structure differs only by one methyl group, with methylated uracil (peak 4) at a retention time of 20.2 min and methylated thymine (peak 5) at a retention time of 21.3 min. In addition, some of the methylated nucleosides were detected directly, including 2'-deoxy-3-methyl-3',5'-di-O-methyl-uridine (peak 10), 2'-deoxy-N,O,O-trimethyl-thymidine (peak 11), and 2'-deoxy-N,O,O,O-tetramethyl-adenosine (peak 12). The detected methylated nucleosides are more stable and their structures are simpler than the other tested nucleosides. Additionally, the mass fragments of the detected nucleosides are within the selected mass range ( $m/z$  40-500) of our analysis.

Figure 7 shows the abundance of methyl furfuryl produced from the TMAH thermochemolysis of nucleoside mixtures at different temperatures. The abundance of methyl furfuryl was relatively consistent from 200 to 500 °C. The abundance of the methylated furfuryl is the highest at 600 °C. This demonstrated that methyl furfuryl is eliminated from the main structure of the nucleosides and detected at 200 °C. With an increase in temperature, the methylated nucleosides are split into two parts: methylated furfuryl and methylated nucleobases. Therefore, the abundance of the methylated nucleosides mixtures decreased with the increase in thermochemolysis temperature, which shows a phenomenon similar to that of individual nucleotides.

### 3.4 SAM-like ramp

We proceeded to TMAH thermochemolysis of nucleosides using a program of temperature of the pyrolyzer starting from 50°C then heating the sample at a 35°C.min<sup>-1</sup> up to 850 °C (the volatiles was trapped in the column inlet) to simulate the way Mars samples are heated in the SAM instrument onboard the Curiosity rover. Figure 8 shows the products from the TMAH thermochemolysis of nucleosides under the SAM-like ramp of pyrolysis. Compared with the chromatogram of nucleosides with TMAH thermochemolysis using a flash pyrolysis (Figure 2), it was found that the methylated compounds of each nucleoside and the byproducts from each nucleoside with TMAH thermochemolysis using a SAM-like ramp pyrolysis are the same.

Figure 9 shows the chromatogram of the mixtures of five kinds of nucleosides with TMAH thermochemolysis under a SAM-like ramp pyrolysis. As discussed previously, dG was not mixed with the other five nucleosides because guanine can decompose into caffeine and influence the quantitation of hypoxanthine. Results showed that there is no overlap of the products among these five nucleosides with TMAH thermochemolysis. The target compounds of each nucleoside with TMAH thermochemolysis is shown in Figure 9. Figure 10 shows the abundance of the target compounds from each nucleoside with TMAH thermochemolysis. When the peak intensities of the target compounds from each nucleoside are compared, the corresponding values of these products as detected by GC/MS decrease in the following manner: dA > dG > dT > dU > dI > dC. These results demonstrate that dA is the most likely to be identified among the tested nucleosides. The result is consistent with the conclusion in our previous work since adenine is the most detectable nucleobase in the context of the limits of detection of GC/MS instrumentation currently used for analysis of martian samples [34].

## 4. Discussion

### 4.1 Methylated nucleobases and nucleosides

The main derivatized compounds of nucleosides are listed in Table 2. Most of the derivatized compounds are the methylated products of six nucleosides, including methylated nucleobases, methylated ribose derivatives, and methylated nucleosides (Figure 11). However,

there are several different methylated products because of the different tautomeric forms of nucleobases.

For dA, there are four possible methylation sites: two are on the nucleobase site and the two others are on the glucose sites. The product of a full methylation of adenosine is 2'-deoxy-N,N,O,O-tetramethyl-adenosine, mainly in N9H form. This demonstrates that the N9H form of adenosine is the most stable form. Both N9H and N3H forms of adenine, the degradation products of adenosine, were detected. The abundance of the N9H form of adenine is higher than the N3H form. This is because the N9H tautomeric form is the major form of adenine while the N3H tautomeric form is the minor form. Moreover, the N9H form of adenine was the most stable tautomer [35,36]. N,9-dimethyl-adenine at low abundance was detected, which is also the methylated derivative of the N9H form of adenine. The relative abundance of trimethylated-adenine is much higher than the dimethylated adenine, because the stability of the trimethylated adenine is higher than the dimethylated one [34].

Trimethyl- and tetramethyl-guanine are the main degradation products from dG with TMAH thermochemolysis. There are several tautomeric methylated products of guanine with the keto and enol forms being the most stable. Methylated 1,3,7-tri-methylxanthine (caffeine) was detected from the TMAH thermochemolysis of dG. This could be caused by the deamination and oxidation of guanine to xanthine, followed by methylation by TMAH.

Methylated dC (2'-deoxy-N,N,O,O-tetramethyl-cytidine) and methylated cytidine are the main products of dC with TMAH thermochemolysis. There are four methylation sites on dC: two sites are on the nucleobase side and two sites are on the glucose side. The thermochemolysis temperature (from 200 to 500°C) had no effect on the number of functionalized derivatives that were detected from dC. However, at 600 °C, the intensity of methylated dC and N,N,N'-trimethyl-cytosine is the highest (excluding the effect of internal standard at 200 °C), which demonstrated that increasing temperature leads to the decomposition of dC. 600 °C will be the optimal temperature for the detection of dC. Compared with other nucleosides tested in this study, the peak intensity of dC is the lowest, so it is more difficult to detect. This is consistent with the properties of cytosine with TMAH thermochemolysis [34].

2'-deoxy-N,O,O-trimethyl-thymidine and 2'-deoxy-3-methyl-3',5'-di-O-methyl-uridine were two of the main methylated products detected from the thermochemolysis of thymidine and uridine with TMAH. Thymidine and uridine produce similar derivatized pyrimidine bases since the molecules differ only by the presence of an extra methyl group at carbon position 5 in thymidine. For thymidine and uridine, the N1 position is the only labile

site of the nucleobase ring, and the active hydrogen of the secondary amine is replaced by a methyl functional group during TMAH thermochemolysis. In addition, the hydrogens of hydroxyl from deoxyribose were methylated by TMAH thermochemolysis. Mainly the canonical forms of methylated thymidine and uridine were detected in this study, because the canonical tautomer of thymine and uracil is thermodynamically more stable than keto, enol and keto-enol tautomerism [37–41]. Therefore, 2'-deoxy-N,O,O-trimethyl-thymidine and 2'-deoxy-3-methyl-3',5'-di-O-methyl-uridine are the main methylated products from dT and dU with TMAH thermochemolysis at low temperature, respectively.

When the temperature of the TMAH thermochemolysis increased from 200 to 500 °C, methylated thymine and uracil were detected as the main products of dU and dT, respectively. This is caused by the thermal degradation of dU and dT, since the C-N sugar-base bond (293 kJ/mol) is one of the thermally weakest bonds in the DNA structure [42]. The canonical forms of methylated thymine and uracil were predominantly detected because the stability of the canonical form is much higher than other forms, and the keto-enolic thermodynamic equilibrium shifted in favor of the formation of the ketone form of uracil and thymine, leading to the absence of the enolactic tautomeric forms of thymine and uracil [37–40,43]. This is similar to the result obtained from the study of nucleobases with TMAH thermochemolysis [34]. The consistency of these results demonstrates that the TMAH thermochemolysis of nucleosides does not influence the additional structure of deoxyribose. When dT and dU were heated, ribose was released from the thymidine and uridine molecules, radicals of thymine and uracil were formed and they were methylated by TMAH. The stability of dT and dU was reduced at high temperature. Thus, methylated thymine and uracil were the main products of thymidine and uridine from TMAH thermochemolysis at 600 °C.

For dI, 1,7-dimethyl-hypoxanthine and methylated dI are the main products. Methylated dI has two forms: 2'-deoxy-3-methyl-3',5'-di-O-methyl-inosine and 2'-deoxy-3-methyl-3',5'-di-O-methyl-hypothanxine. This could be caused by the oxidation of hypoxanthine. An increasing thermochemolysis temperature leads to the degradation of dI, forming methylated hypothanxine and furfuryl methyl ether.

#### 4.2 The formation of furan derivatives

2-(methoxymethyl)furan and 3-methoxy-2-(methoxymethyl)-2,3-dihydrofuran are also the main methylated products from the TMAH thermochemolysis of nucleosides. 3-methoxy-2-(methoxymethyl)-2,3-dihydrofuran is the methylated product of 2-(hydroxymethyl)-2,3-

dihydrofuran-3-ol, which is the product formed from the degradation of the nucleoside. Furfuryl alcohol is the product of 3-methoxy-2-(methoxymethyl)-2,3-dihydrofuran under dehydration. 2-(methoxymethyl)furan is formed when the hydrogen from the hydroxyl group of the furfuryl alcohol is replaced by the methyl functional group of TMAH. The abundance of 2-(methoxymethyl)furan was higher than that of 3-methoxy-2-(methoxymethyl)-2,3-dihydrofuran, which demonstrated that the structure of 2-(methoxymethyl)furan was more stable than 3-methoxy-2-(methoxymethyl)-2,3-dihydrofuran.

Deoxyribose and ribose generated by dihydrogen abstraction are important intermediates in radiation damage [44]. It is known that the furanose ring is puckered rather than planar [45]. The furanose molecule has relatively high internal energy because of this twisted molecular structure, and there are no  $\pi$ -electrons in the furanose molecule. Therefore, it is easier for furanose to be decomposed. Neutral  $C_5H_6O_2$  was proven to be one of the important products of thermal decomposition of deoxyribose [46]. The products of the dissociative electron attachment cross sections for the three heaviest fragment anions are  $C_5H_9O_4$ ,  $C_5H_7O_3$ , and  $C_5H_6O_2$  [46]. This demonstrated that  $C_5H_7O_3$ , and  $C_5H_6O_2$  could be the main radicals of the deoxyribose component of nucleosides under thermochemolysis at temperatures higher than 200 °C. Therefore, 2-(methoxymethyl)furan and 3-methoxy-2-(methoxymethyl)-2,3-dihydrofuran are the main products from the degradation of the deoxyribose component of nucleosides.

## 5. Conclusions

The products of nucleosides with TMAH thermochemolysis were studied under flash pyrolysis and a SAM-like ramp pyrolysis. We conclude that the methylated nucleobases are the main compounds of nucleosides with TMAH thermochemolysis. The optimal temperature for the detection of methylated nucleosides is 200 °C; for methylated nucleobases and ribose derivatives such as furfuryl methyl ether is 600 °C. The structure of the original DNA/RNA fragments influence the detection of the characteristic compounds. For example, the abundance of methylated nucleosides following TMAH thermochemolysis of the tested nucleosides can vary substantially. However, the optimal temperature can be different if the nucleoside is contained within some solid matrix. A higher thermochemolysis temperature can aid in the detection of nucleosides by enabling a higher efficiency of desorption. Nucleobases are the main products of nucleosides with TMAH thermochemolysis and the

limit of detection has been reported in our previous work [34]. Though some of the thermochemolysis products may not be detected, a thermochemolysis temperature of 600 °C still enables the detection of diagnostic products of nucleosides with TMAH thermochemolysis, which is consistent with thermochemolysis temperatures that will be applied on SAM and MOMA. These results demonstrate that the temperature of TMAH thermochemolysis affects the efficiency of the detection of DNA fragments. If there are indications of past or present life on Mars at the surface or near subsurface in the form of molecular fragments analogous to DNA, the experimental conditions of life detection instrumentation should be further optimized in the future.

## Acknowledgement

This work was supported by CNES, focused on Sample Analysis at Mars of the Mars Science Laboratory mission, and Mars Organic Molecules Analyzer of the Exomars 2022 mission. Y.H. was supported by the CSC scholarship (201701810036). We thank Vincent Butin and Jamila El Bekri for their help in experimental setup.

## Declaration of Competing Interest

No competing interests exist.

## References

- [1] A.J. Williams, J. Eigenbrode, M. Floyd, M.B. Wilhelm, S. O'Reilly, S.S. Johnson, K.L. Craft, C.A. Knudson, S. Andrejkovičová, J.M.T. Lewis, A. Buch, D.P. Glavin, C. Freissinet, R.H. Williams, C. Szopa, M. Millan, R.E. Summons, A. McAdam, K. Benison, R. Navarro-González, C. Malespin, P.R. Mahaffy, Recovery of fatty acids from mineralogic Mars analogs by TMAH thermochemolysis for the Sample Analysis at Mars wet chemistry experiment on the Curiosity Rover, *Astrobiology*. 19 (2019) 522–546. <https://doi.org/10.1089/ast.2018.1819>.
- [2] F. Stalport, D.P. Glavin, J.L. Eigenbrode, D. Bish, D. Blake, P. Coll, C. Szopa, A. Buch, A. McAdam, J.P. Dworkin, P.R. Mahaffy, The influence of mineralogy on recovering organic acids from Mars analogue materials using the one-pot derivatization experiment on the Sample Analysis at Mars (SAM) instrument suite, *Planet. Space Sci.* 67 (2012) 1–13. <https://doi.org/10.1016/j.pss.2012.02.010>.
- [3] B.R.T. Simoneit, Molecular indicators (biomarkers) of past life, *Anat. Rec.* 268 (2002) 186–195. <https://doi.org/10.1002/ar.10153>.
- [4] B.R.T. Simoneit, R.E. Summons, L.L. Jahnke, Biomarkers as tracers for life on early Earth and Mars, *Orig. Life Evol. Biosph.* 28 (1998) 475–483. <https://doi.org/10.1023/a:1006508012904>.

- [5] G. Dandanell, B. Hove-Jensen, M. WillemoËs, K.F. Jensen, Nucleotides, Nucleosides, and Nucleobases, *EcoSal Plus*. 3 (2008). <https://doi.org/10.1128/ecosalplus.3.6.2>.
- [6] K.A. Jacobson, M.F. Jarvis, M. Williams, Purine and pyrimidine (P2) receptors as drug targets, *J. Med. Chem.* 45 (2002) 4057–4093. <https://doi.org/10.1021/jm020046y>.
- [7] Y. Dong, F. Sun, Z. Ping, Q. Ouyang, L. Qian, DNA storage : research landscape and future prospects, *Natl. Sci. Rev.* (2020) 0–1.
- [8] B.K.D. Pearce, R.E. Pudritz, D.A. Semenov, T.K. Henning, Origin of the RNA world: The fate of nucleobases in warm little ponds, *Proc. Natl. Acad. Sci. U. S. A.* 114 (2017) 11327–11332. <https://doi.org/10.1073/pnas.1710339114>.
- [9] A. Biscans, Exploring the emergence of RNA nucleosides and nucleotides on the early earth, *Life*. 8 (2018). <https://doi.org/10.3390/life8040057>.
- [10] D.M. Fialho, K.C. Clarke, M.K. Moore, G.B. Schuster, R. Krishnamurthy, N. V. Hud, Glycosylation of a model proto-RNA nucleobase with non-ribose sugars: Implications for the prebiotic synthesis of nucleosides, *Org. Biomol. Chem.* 16 (2018) 1263–1271. <https://doi.org/10.1039/c7ob03017g>.
- [11] C. Menor-Salván, From the Dawn of Organic Chemistry to Astrobiology: Urea as a Foundational Component in the Origin of Nucleobases and Nucleotides, in: 2018: pp. 85–142. [https://doi.org/10.1007/978-3-319-93584-3\\_4](https://doi.org/10.1007/978-3-319-93584-3_4).
- [12] V.A. Basiuk, J. Doua, Pyrolysis of simple amino acids and nucleobases: survivability limits and Implications for extraterrestrial delivery, *Planet. Space Sci.* 47 (1999) 577–584. [https://doi.org/10.1016/S0032-0633\(98\)00136-6](https://doi.org/10.1016/S0032-0633(98)00136-6).
- [13] D.B. Davies, Conformations of nucleosides and nucleotides, *Prog. Nucl. Magn. Reson. Spectrosc.* 12 (1978) 135–225. [https://doi.org/10.1016/0079-6565\(78\)80006-5](https://doi.org/10.1016/0079-6565(78)80006-5).
- [14] S. Steenken, Purine Bases, Nucleosides, and Nucleotides: Aqueous Solution Redox Chemistry and Transformation Reactions of Their Radical Cations and e<sup>-</sup> and OH Adducts, *Chem. Rev.* 89 (1989) 503–520. <https://doi.org/10.1021/cr00093a003>.
- [15] C. Altona, M. Sundaralingam, Conformational analysis of the sugar ring in nucleosides and nucleotides. Improved method for the interpretation of proton magnetic resonance coupling constants, *J. Am. Chem. Soc.* 95 (1973) 2333–2344. <https://doi.org/10.1021/ja00788a038>.
- [16] G.A. Jeffrey, H. Maluszynska, J. Mitra, Hydrogen bonding in nucleosides and nucleotides, *Int. J. Biol. Macromol.* 7 (1985) 336–348. [https://doi.org/10.1016/0141-8130\(85\)90048-0](https://doi.org/10.1016/0141-8130(85)90048-0).
- [17] R. Saladino, J.E.J.J.E. Šponer, J.E.J.J.E. Šponer, G. Costanzo, S. Pino, E. Di Mauro, Chemomimesis and molecular darwinism in action: From abiotic generation of nucleobases to nucleosides and RNA, *Life*. 8 (2018) 1–15. <https://doi.org/10.3390/life8020024>.
- [18] R. Saladino, B.M. Bizzarri, L. Botta, J. Šponer, J.E. Šponer, T. Georgelin, M. Jaber, B. Rigaud, M. Kapralov, G.N. Timoshenko, A. Rozanov, E. Krasavin, A.M. Timperio, E. Di Mauro, Proton irradiation: A key to the challenge of N-glycosidic bond formation in a prebiotic context, *Sci. Rep.* 7 (2017) 8–15. <https://doi.org/10.1038/s41598-017-15392-8>.
- [19] Y. Furukawa, H.J. Kim, D. Hutter, S.A. Benner, Abiotic regioselective phosphorylation of adenosine with borate in formamide, *Astrobiology*. 15 (2015) 259–267. <https://doi.org/10.1089/ast.2014.1209>.
- [20] M. V. Dubina, S.Y. Vyazmin, V.M. Boitsov, E.N. Nikolaev, I.A. Popov, A.S. Kononikhin, I.E. Eliseev, Y. V. Natchin, Potassium Ions are More Effective than Sodium Ions in Salt Induced



- Peptide Formation, *Orig. Life Evol. Biosph.* 43 (2013) 109–117.  
<https://doi.org/10.1007/s11084-013-9326-5>.
- [21] Y. Sheng, H.D. Bean, I. Mamajanov, N. V. Hud, J. Leszczynski, Comprehensive investigation of the energetics of pyrimidine nucleoside formation in a model prebiotic reaction, *J. Am. Chem. Soc.* 131 (2009) 16088–16095. <https://doi.org/10.1021/ja900807m>.
- [22] E.Y. Aguilar-Ovando, A. Negron-Mendoza, Radiolysis of Nucleosides: Study of Sedimentary Microenvironment Models for the Protection of Bio-Organic Molecules on Early Earth, *J. Nucl. Physics, Mater. Sci. Radiat. Appl.* 5 (2017) 103–111. <https://doi.org/10.15415/jnp.2017.51010>.
- [23] F. Cataldo, Radiolysis and radioracemization of RNA ribonucleosides: implications for the origins of life, *J. Radioanal. Nucl. Chem.* 318 (2018) 1649–1661.  
<https://doi.org/10.1007/s10967-018-6276-4>.
- [24] M.P. Callahan, K.E. Smith, H.J. Cleaves, J. Ruzicka, J.C. Stern, D.P. Glavin, C.H. House, J.P. Dworkin, Carbonaceous meteorites contain a wide range of extraterrestrial nucleobases, *Proc. Natl. Acad. Sci. U. S. A.* 108 (2011) 13995–13998. <https://doi.org/10.1073/pnas.1106493108>.
- [25] B.K.D. Pearce, R.E. Pudritz, Seeding the Pregenetic Earth: Meteoritic Abundances of Nucleobases and Potential Reaction Pathways, *Astrophys. J.* 807 (2015) 85.  
<https://doi.org/10.1088/0004-637X/807/1/85>.
- [26] Z. Martins, O. Botta, M.L. Fogel, M.A. Sephton, D.P. Glavin, J.S. Watson, J.P. Dworkin, A.W. Schwartz, P. Ehrenfreund, Extraterrestrial nucleobases in the Murchison meteorite, *Earth Planet. Sci. Lett.* 270 (2008) 130–136. <https://doi.org/10.1016/j.epsl.2008.03.026>.
- [27] Y. Oba, Y. Takano, H. Naraoka, Y. Furukawa, D.P. Glavin, J.P. Dworkin, S. Tachibana, Extraterrestrial hexamethylenetetramine in meteorites—a precursor of prebiotic chemistry in the inner solar system, *Nat. Commun.* 11 (2020) 1–8. <https://doi.org/10.1038/s41467-020-20038-x>.
- [28] J.P.D. & H.N. Yasuhiro Oba, Yoshinori Takano, Yoshihiro Furukawa, Toshiki Koga, Daniel P. Glavin, Identifying the wide diversity of extraterrestrial purine and pyrimidine nucleobases in carbonaceous meteorites, *Nat. Commun.* 2008 (2022).
- [29] Y. Furukawa, Y. Chikaraishi, N. Ohkouchi, N.O. Ogawa, D.P. Glavin, J.P. Dworkin, C. Abe, T. Nakamura, Extraterrestrial ribose and other sugars in primitive meteorites, *Proc. Natl. Acad. Sci. U. S. A.* 116 (2019) 24440–24445. <https://doi.org/10.1073/pnas.1907169116>.
- [30] S.A. Villafañe-Barajas, J.P.T. Baú, M. Colín-García, A. Negrón-Mendoza, A. Heredia-Barbero, T. Pi-Puig, D.A.M. Zaia, Salinity Effects on the Adsorption of Nucleic Acid Compounds on Na-Montmorillonite: a Prebiotic Chemistry Experiment, *Orig. Life Evol. Biosph.* 48 (2018) 181–200. <https://doi.org/10.1007/s11084-018-9554-9>.
- [31] L.A. Leshin, P.R. Mahaffy, C.R. Webster, M. Cabane, P. Coll, P.G. Conrad, P.D. Archer, S.K. Atreya, A.E. Brunner, A. Buch, J.L. Eigenbrode, G.J. Flesch, H.B. Franz, C. Freissinet, D.P. Glavin, A.C. McAdam, K.E. Miller, D.W. Ming, R. V. Morris, R. Navarro-González, P.B. Niles, T. Owen, R.O. Pepin, S. Squyres, A. Steele, J.C. Stern, R.E. Summons, D.Y. Sumner, B. Sutter, C. Szopa, S. Teinturier, M.G. Trainer, J.J. Wray, J.P. Grotzinger, Volatile, isotope, and organic analysis of martian fines with the Mars curiosity rover, *Science* (80-. ). 341 (2013) 1238937. <https://doi.org/10.1126/science.1238937>.
- [32] Y. He, A. Buch, C. Szopa, A.J. Williams, M. Millan, C.A. Malespin, D.P. Glavin, C. Freissinet, J.L. Eigenbrode, S. Teinturier, D. Coscia, J.Y. Bonnet, J.C. Stern, F. Stalport, M. Guzman, N. Chaouche-Mechidal, P. Lu, R. Navarro-gonzalez, V. Butin, J. El Bekri, H. Cottin, S. Johnson, M. Cabane, P.R. Mahaffy, J. El Bekri, S. Johnson, M. Cabane, P.R. Mahaffy, Influence of

- Calcium Perchlorate on the Search for Organics on Mars with Tetramethylammonium Hydroxide Thermochemolysis, *Astrobiology*. 21 (2021) 1–19. <https://doi.org/10.1089/ast.2020.2252>.
- [33] Y. He, A. Buch, C. Szopa, M. Millan, C. Freissinet, R. Navarro-Gonzalez, M. Guzman, S. Johnson, D. Glavin, A. Williams, J. Eigenbrode, S. Teinturier, C. Malespin, D. Coscia, J.-Y. Bonnet, P. Lu, M. Cabane, P. Mahaffy, Influence of Calcium Perchlorate on the Search for Martian Organic Compounds with MTBSTFA/DMF Derivatization, *Astrobiology*. 21 (2021) 1137–1156. <https://doi.org/10.1089/ast.2020.2393>.
- [34] Y. He, A. Buch, M. Morisson, C. Szopa, C. Freissinet, A. Williams, M. Millan, M. Guzman, R. Navarro-Gonzalez, J.Y. Bonnet, D. Coscia, J.L. Eigenbrode, C.A. Malespin, P. Mahaffy, D.P. Glavin, J.P. Dworkin, P. Lu, S.S. Johnson, Application of TMAH thermochemolysis to the detection of nucleobases: Application to the MOMA and SAM space experiment, *Talanta*. 204 (2019) 802–811. <https://doi.org/10.1016/j.talanta.2019.06.076>.
- [35] C. Fonseca Guerra, F.M. Bickelhaupt, S. Sana, F. Wang, Adenine tautomers: Relative stabilities, ionization energies, and mismatch with cytosine, *J. Phys. Chem. A*. 110 (2006) 4012–4020. <https://doi.org/10.1021/jp057275r>.
- [36] M. Hanus, M. Kabeláč, J. Rejnek, F. Ryjáček, P. Hobza, Correlated ab Initio Study of Nucleic Acid Bases and Their Tautomers in the Gas Phase, in a Microhydrated Environment, and in Aqueous Solution. Part 3. Adenine, *J. Phys. Chem. B*. 108 (2004) 2087–2097. <https://doi.org/10.1021/jp036090m>.
- [37] M.A. Morsy, A.M. Al-Somali, A. Suwaiyan, Fluorescence of Thymine Tautomers at Room Temperature in Aqueous Solutions, *J. Phys. Chem. B*. 103 (1999) 11205–11210. <https://doi.org/10.1021/jp990858e>.
- [38] M.K. Shukla, J. Leszczynski, Interaction of water molecules with cytosine tautomers: An excited-state quantum chemical investigation, *J. Phys. Chem. A*. 106 (2002) 11338–11346. <https://doi.org/10.1021/jp021317j>.
- [39] Y. Tsuchiya, T. Tamura, M. Fujii, M. Ito, Keto-enol tautomer of uracil and thymine, *J. Phys. Chem.* 92 (1988) 1760–1765. <https://doi.org/10.1021/j100318a013>.
- [40] B.B. Brady, L.A. Peteanu, D.H. Levy, The electronic spectra of the pyrimidine bases uracil and thymine in a supersonic molecular beam, *Chem. Phys. Lett.* 147 (1988) 538–543. [https://doi.org/10.1016/0009-2614\(88\)80264-1](https://doi.org/10.1016/0009-2614(88)80264-1).
- [41] Rejnek, J., Hanus, M., Kabeláč, M., Ryjáček, F., & Hobza, P., Correlated ab initio study of nucleic acid bases and their tautomers in the gas phase, in a microhydrated environment and in aqueous solution : Part 4. Uracil and thymine, *Phys. Chem. Chem. Phys.* 7 (2005) 2006–2017. <https://doi.org/10.1039/B202156K>.
- [42] J. Alongi, A. Di Blasio, J. Milnes, G. Malucelli, S. Bourbigot, B. Kandola, G. Camino, Thermal degradation of DNA, an all-in-one natural intumescent flame retardant, *Polym. Degrad. Stab.* 113 (2015) 110–118. <https://doi.org/10.1016/j.polymdegradstab.2014.11.001>.
- [43] J. Rejnek, M. Hanus, M. Kabeláč, F. Ryjáček, P. Hobza, Correlated ab initio study of nucleic acid bases and their tautomers in the gas phase, in a microhydrated environment and in aqueous solution. Part 3. Adenine, *Phys. Chem. Chem. Phys.* 108 (2004) 2087–2097. <https://doi.org/10.1039/B501499A>.
- [44] R. Téoule, Radiation-induced DNA damage and its repair, *Int. J. Radiat. Biol.* 51 (1987) 573–589. <https://doi.org/10.1080/09553008414552111>.
- [45] S. Denifl, S. Matejčík, B. Gstir, G. Hanel, M. Probst, P. Scheier, T.D. Märk, *Electron*

attachment to 5-chloro uracil, *J. Chem. Phys.* 118 (2003) 4107–4114.  
<https://doi.org/10.1063/1.1540108>.

- [46] S. Ptasińska, S. Denifl, P. Scheier, T.D. Märk, Inelastic electron interaction (attachment/ionization) with deoxyribose, *J. Chem. Phys.* 120 (2004) 8505–8511.  
<https://doi.org/10.1063/1.1690231>.

Journal Pre-proof

**Figure captions:**

**Figure 1** Skeletal formulae of selected nucleobases and nucleosides. dA, deoxyadenosine; dG, deoxyguanosine; dC, 2'-deoxycytidine; dT, thymidine; dU, 2'-deoxyuridine; dI, deoxy-inosine.

**Figure 2** Chromatograms of the chemical compounds detected after the thermochemolysis of nucleosides with TMAH at flash pyrolysis of 200 °C. The signal plotted is the total ion current of the MS detector. IS stands for internal standard (Naphthalene-D8). **dI** peak 1: Furfuryl ether, RT=6.1 min; 2:Caffeine, RT=26.9min; 3: 1,7-dimethyl hypoxanthine and isomers, RT=27.5 and 28.6 min; 4: 2'-deoxy-3-methyl-3',5'-di-O-methyl-inosine, RT=32.65 min. **dC** peak 1: Furfuryl ether, RT=6.1 min; 2: 4-Dimethylamino-1-methyl-2(1H)-pyrimidinone and isomers, RT=27.4 min; 3: 2'-deoxy-N,N,O,O-tetramethyl- Cytidine, RT=34.4 min; **dU** peak 1: Furfuryl ether, RT=6.1 min; 2: 1,3-dimethyl-uracil; RT=20.2 min; 3: 2'-Deoxy-3-methyl-3',5'-di-O-methyl-uridine and isomers. **dT** peak 1: Furfuryl ether, RT=6.1 min; 3: 1,3-Dimethyl-thymidine; RT= 21.5 min. **dG** peak 1: Furfuryl ether, RT=6.1 min; 2: Caffeine, RT=27.0 min; 3: trimethyl-guanine, RT=28.0 min; 4: Tetramethyl-guanine, RT=29.14 min; 5: Methyl guanosine and isomers, RT=34.5 min. **dA** Peak 1: Furfuryl ether, RT=6.1 min; 2: N,9-dimethyl-9H-Purin-6-amine or N,9-dimethyl-adenine, RT=25.0 min; 3: N,N,9-Trimethyl-9H-purin-6-amine or N,N,9-Trimethyl-adenine and isomers, RT=25.9 min; 4: N,N,3-Trimethyl-9H-purin-6-amine or N,N,3-Trimethyl-adenine and isomers, RT=26.8 min; 5: 2'-deoxy-N,N,O,O-tetramethyl-adenosine and isomers, RT=33.1 min.

**Figure 3** Mass spectrum of the organic compounds from nucleosides with TMAH thermochemolysis. The information of each molecule fragment has been listed in the supplementary material (Table S7).

**Figure 4** Chromatograms of the chemical compounds detected after the TMAH thermochemolysis of nucleosides for the different flash pyrolysis temperatures studied. The signal plotted is the total ion current of the MS detector. IS stands for internal standard (Naphthalene-D8). dA: 1: 2-methoxymethyl-Furan; 2: 3-methoxy-2-(methoxymethyl)-2,3-dihydrofuran; 3: 2,3-diethyl-5-methyl-Pyrazine; 4: N,N,9-Trimethyl-adenine; 5: N,N,3-trimethyl-adenine; 6: 2'-deoxy-N,NO,O-tetramethyl-adenosine. dG: 1: 2-methoxymethyl-Furan; 2: Caffeine;3: Hexadecanoic acid methyl ester; 4 and 5:Tetramethyl-guanine and isomers. dT: 1 and 2: 2-methoxymethyl-Furan ;3: 1,3-Dimethyl-thymidine; 4: 2'-deoxy-N,N,O-trimethyl- thymidine. dU:1 and 2: 2-methoxymethyl-Furan and isomers; 3: 1,3-dimethyl-uracil; 4: 2'-Deoxy-3-methyl-3',5'-di-O-methyl-Uridine. dC:1 and 2: 2-methoxymethyl-Furan and isomers; 3: 4-Dimethylamino-1-methyl-2(1H)-pyrimidinone and isomers; 4: 2'-deoxy-N,N,O,O-tetramethyl- Cytidine. dI: 1 and 2: 2-methoxymethyl-Furan and isomers; 3 and 4: 1,7-Dimethyl-hypoxanthine and isomers.

**Figure 5** Evolution of the amount of the main products detected after TMAH thermochemolysis of nucleosides at different temperatures ( $A_i/A_{IS}$  is the ratio of the area of an organic chromatographic peak and the area of the internal standard chromatographic peak). The signal plotted is the total ion current of the MS detector. IS stands for internal standard (Naphthalene-D8).

**Figure 6** Chromatograms of the chemical compounds detected after TMAH thermochemolysis of the mixture of nucleosides (10 nmol) at different temperatures. The signal plotted is the total ion current of the MS detector. IS stands for internal standard (Naphthalene-D8, RT=15.3 min). Peak 1 : RT=6.1 min, Furfuryl methyl ether; Peak 2 : RT=10.8 min, 2'-deoxy-Cytidine?; Peak 3 : RT=13.0 min, 3-

methyl-1,2-cyclopentanedione?; Peak 4 : RT=20.1 min, 1,3-dimethyl-uracil ; Peak 5 : RT=21.2 min, 1,3-dimethyl-thymine; Peak 6: RT=25.4 min, N,N,9-trimethyl-adenine; peak 7,9: RT=27.4 and 28.6 min, 1,7-dimethyl-hypoxanthine; peak 8: RT=28.1 min, N,N,3-trimethyl-adenine; peak 10: RT=30.0 min, 2'-deoxy-3-methyl-3',5'-di-O-methyl-Uridine; peak 11: RT=30.44 min, 2'-deoxy-N,O,O-trimethyl-thymidine ; peak 12 : RT=33.0 min, 2'-deoxy-N,O,O,O- tetramethyl-Adenosine.

**Figure 7** Abundance of methyl furfuryl detected after TMAH thermochemolysis of nucleosides at different temperatures ( $A_i/A_{IS}$  is the ratio of the chromatographic peak area of 2-methoxymethyl-furan and the chromatographic peak area of the internal standard).

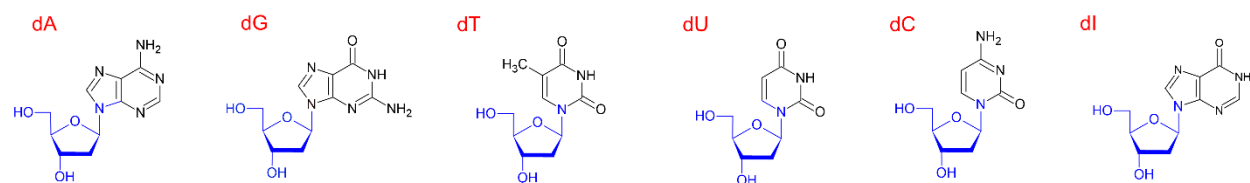
**Figure 8** Chromatograms of the products of TMAH thermochemolysis of nucleosides under a SAM-like ramp pyrolysis. The signal plotted is the total ion current of the MS detector. IS stands for internal standard (Naphthalene-D8).

**Figure 9** The chromatogram following a SAM-like ramp pyrolysis of the mixture of nucleosides. Peak 1: Furfuryl methyl ether; 2: 1,3-dimethyl-uracil; 3: 1,3-dimethyl- thymine; 4: trimethyl-cytosine; 5: N,N,9-Trimethyl-adenine; 6,8: 1,7-dimethyl-hypoxanthine; 7: N,N,3-Trimethyl-adenine; 9: 2'-Deoxy-3-methyl-3',5'-di-O-methyl-Uridine; 10: 2'-Deoxy-3-methyl-3',5'-di-O-methyl-Thymidine; 11: 2'-deoxy-N,N,O,O-tetramethyl-adenosine; 12: 2'-deoxy-N,N,O,O-tetramethyl-cytidine. IS stands for internal standard (Naphthalene-D8).

**Figure 10** The abundance of each methylated nucleoside detected by Py-GC/MS under a SAM-like ramp pyrolysis with TMAH thermochemolysis.

**Figure 11** The TMAH thermochemolysis schemes of six nucleosides.

## Deoxyribo-nucleosides



## Nucleobases

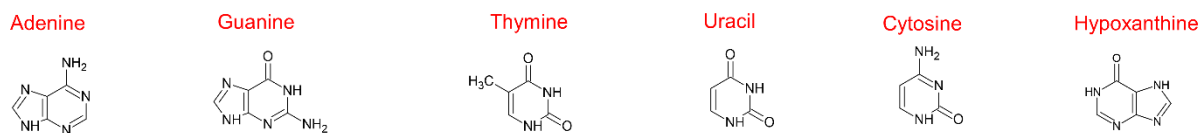


Figure 1 Skeletal formulae of selected nucleobases and nucleosides. dA, deoxyadenosine; dG, deoxyguanosine; dC, 2'-deoxycytidine; dT, thymidine; dU, 2'-deoxyuridine; dI, deoxy-inosine.

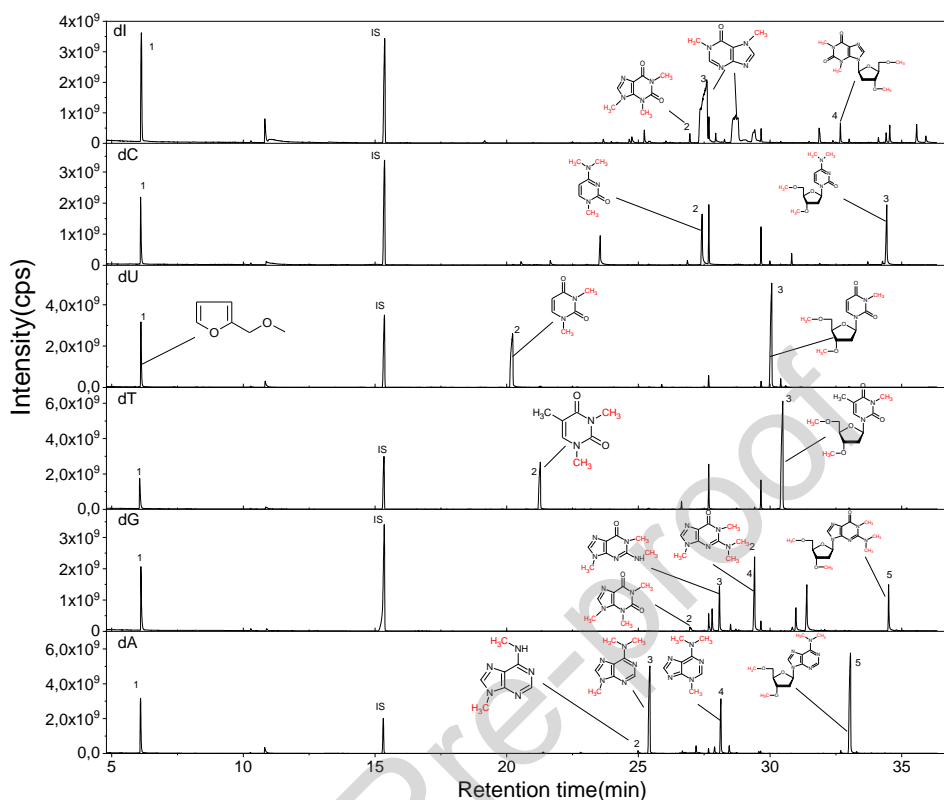


Figure 2 Chromatograms of the chemical compounds detected after the thermochemolysis of nucleosides with TMAH at flash pyrolysis of 200 °C. The signal plotted is the total ion current of the MS detector. IS stands for internal standard (Naphthalene-D8). **dI** peak 1: Furfuryl methyl ether, RT=6.1 min; 2:Caffeine, RT=26.9min; 3: 1,7-dimethyl hypoxanthine and isomers, RT=27.5 and 28.6 min; 4: 2'-deoxy-3-methyl-3',5'-di-O-methyl-inosine, RT=32.65 min. **dC** peak 1: Furfuryl ether, RT=6.1 min; 2: 4-Dimethylamino-1-methyl-2(1H)-pyrimidinone and isomers, RT=27.4 min; 3: 2'-deoxy-N,N,O,O-tetramethyl- Cytidine, RT=34.4 min; **dU** peak 1: Furfuryl ether, RT=6.1 min; 2: 1,3-dimethyl-uracil; RT=20.2 min; 3: 2'-Deoxy-3-methyl-3',5'-di-O-methyl-uridine and isomers, RT=30.0 min; **dT** peak 1: Furfuryl ether, RT=6.1 min; 3: 1,3-Dimethyl-thymidine; RT= 21.5 min. **dG** peak 1: Furfuryl ether, RT=6.1 min; 2: Caffeine, RT=27.0 min; 3: trimethyl-guanine, RT=28.0 min; 4: Tetramethyl-guanine, RT=29.14 min; 5: Methyl guanosine and isomers, RT=34.5 min. **dA** Peak 1: Furfuryl ether, RT=6.1 min; 2: N,9-dimethyl-9H-Purin-6-amine or N,9-dimethyl-adenine, RT=25.0 min; 3: N,N,9-Trimethyl-9H-purin-6-amine or N,N,9-Trimethyl-adenine and isomers, RT=25.9 min; 4: N,N,3-Trimethyl-9H-purin-6-amine or N,N,3-Trimethyl-adenine and isomers, RT=26.8 min; 5: 2'-deoxy-N,N,O,O-tetramethyl-adenosine and isomers, RT=33.1 min.

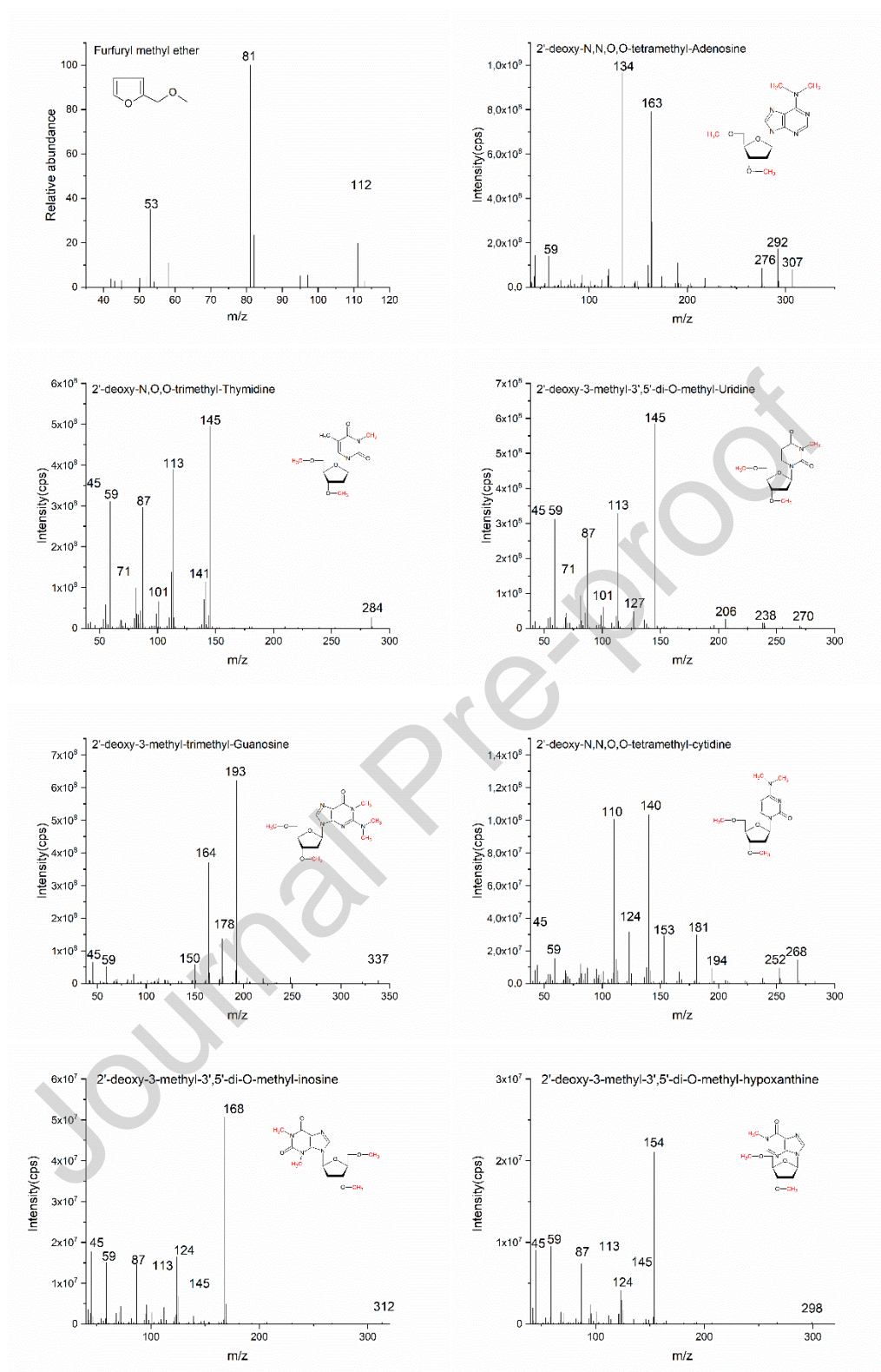


Figure 3 Mass spectrum of the organic compounds from nucleosides with TMAH thermochemolysis. The information of each molecule fragment has been listed in the supplementary material (Table S2).



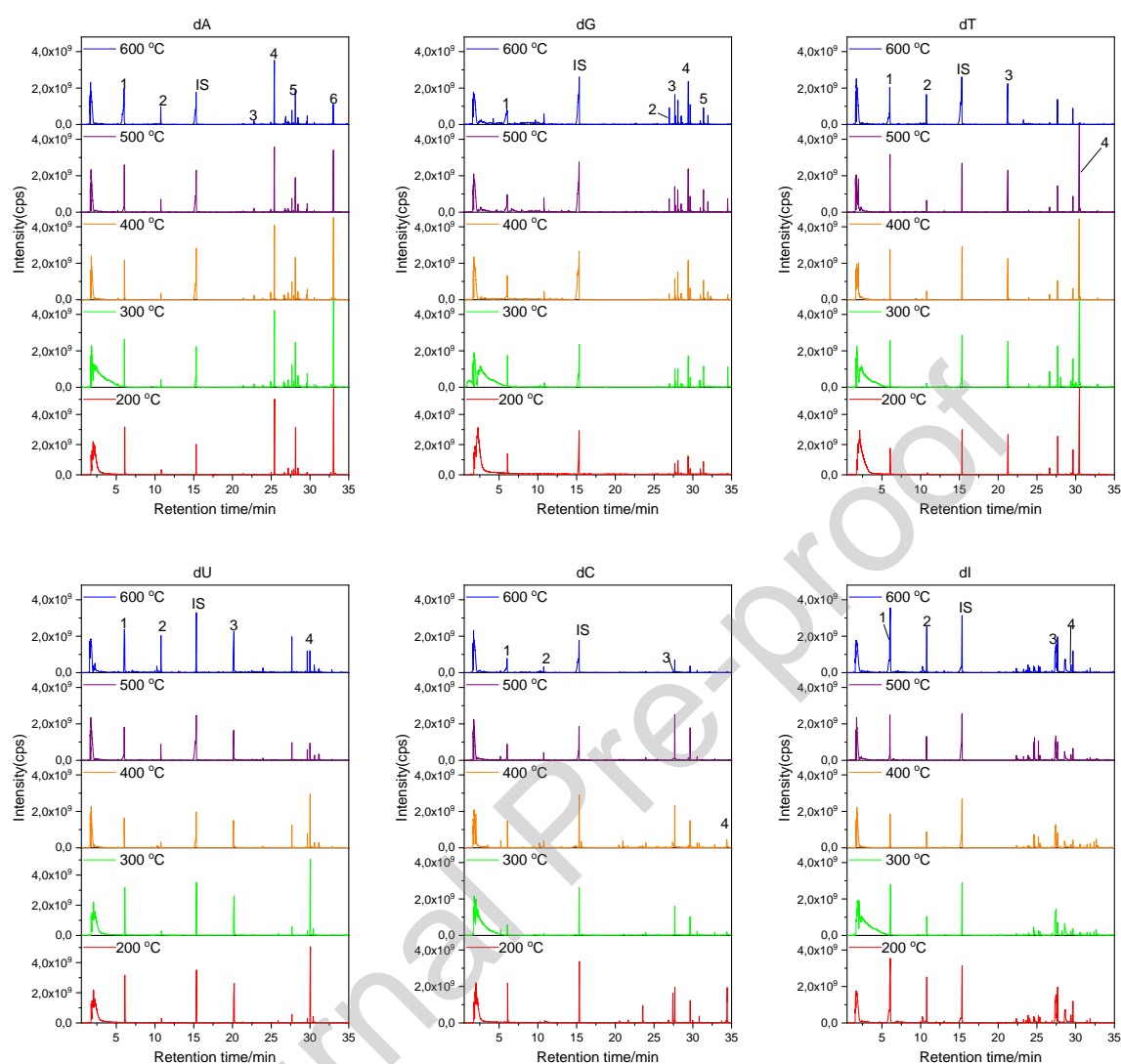


Figure 4 Chromatograms of the chemical compounds detected after the TMAH thermochemolysis of nucleosides for the different flash pyrolysis temperatures studied. The signal plotted is the total ion current of the MS detector. IS stands for internal standard (Naphthalene-D8). **dA**: 1: 2-methoxymethyl-Furan; 2: 3-methoxy-2-(methoxymethyl)-2,3-dihydrofuran; 3: 2,3-diethyl-5-methyl- Pyrazine; 4: N,N,9-Trimethyl-adenine; 5: N,N,3-trimethyl-adenine; 6: 2'-deoxy-N,N,O-tetramethyl-adenosine. **dG**: 1: 2-methoxymethyl-Furan; 2: Caffeine; 3: Hexadecanoic acid methyl ester; 4 and 5: Tetramethyl-guanine and isomers. **dT**: 1 and 2: 2-methoxymethyl-Furan ; 3: 1,3-Dimethyl-thymidine; 4: 2'-deoxy-N,N,O-trimethyl- thymidine. **dU**: 1 and 2: 2-methoxymethyl-Furan and isomers; 3: 1,3-dimethyl-uracil; 4: 2'-Deoxy-3-methyl-3',5'-di-O-methyl-Uridine. **dC**: 1 and 2: 2-methoxymethyl-Furan and isomers; 3: 4-Dimethylamino-1-methyl-2(1H)-pyrimidinone and isomers; 4: 2'-deoxy-N,N,O,O-tetramethyl- Cytidine. **dI**: 1 and 2: 2-methoxymethyl-Furan and isomers; 3 and 4: 1,7-Dimethyl-hypoxanthine and isomers. The peaks at the beginning of the chromatogram are the solvent peak.

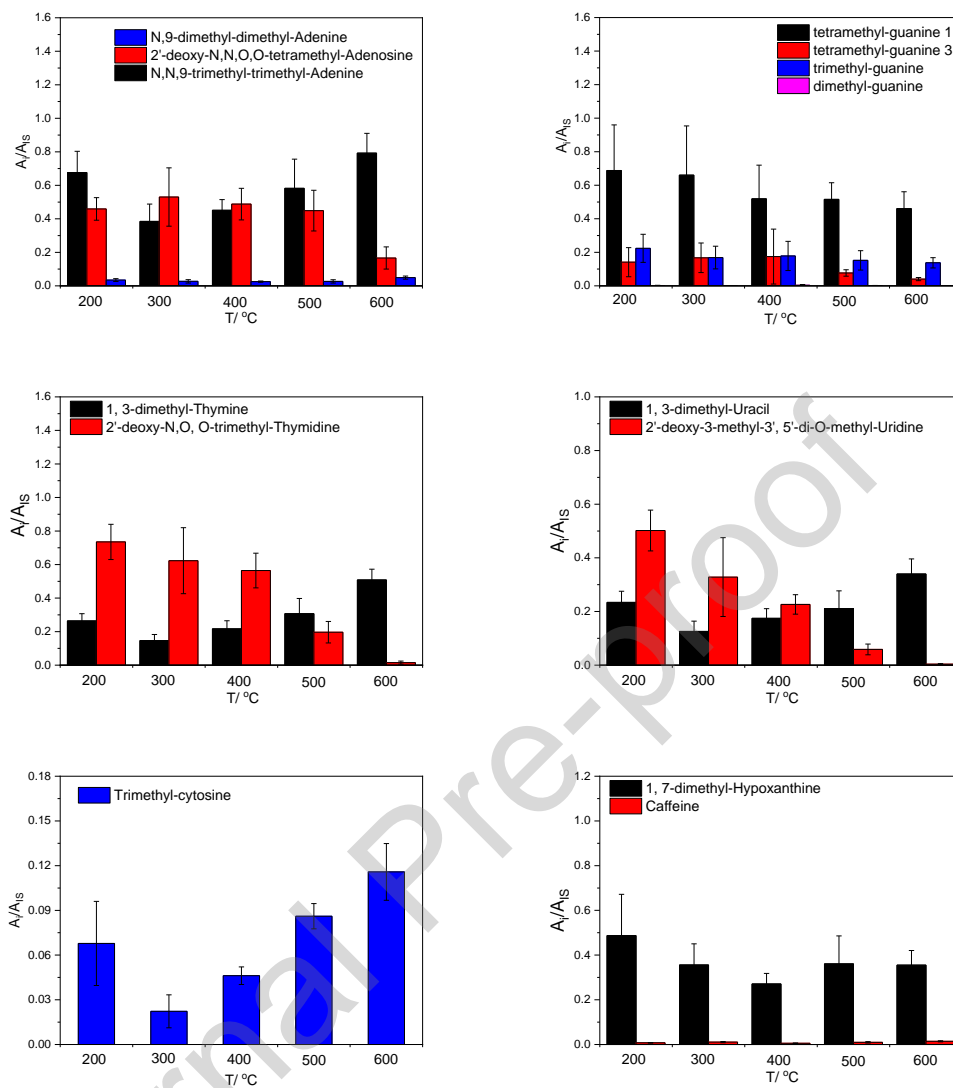


Figure 5 Evolution of the amount of the main products detected after TMAH thermochemolysis of nucleosides at different temperatures ( $A_i/A_{IS}$  is the ratio of the area of an organic chromatographic peak and the area of the internal standard chromatographic peak). The signal plotted is the total ion current of the MS detector. IS stands for internal standard (Naphthalene-D8).

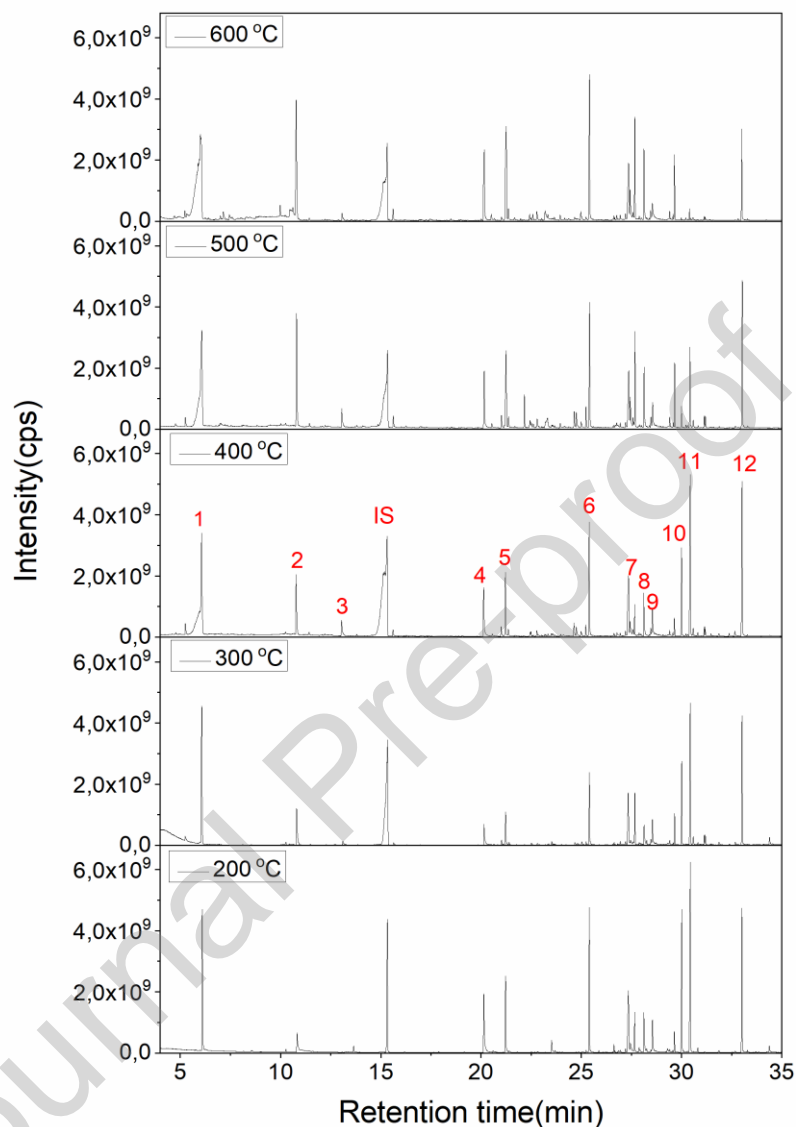


Figure 6 Chromatograms of the chemical compounds detected after TMAH thermochemolysis of the mixture of nucleosides (10 nmol) at different temperatures. The signal plotted is the total ion current of the MS detector. IS stands for internal standard (Naphthalene-D8, RT=15.3 min). Peak 1 : RT=6.1 min, Furfuryl methyl ether; Peak 2 : RT=10.8 min, 2'-deoxy-Cytidine?; Peak 3 : RT=13.0 min, 3-methyl-1,2-cyclopentanedione?; Peak 4 : RT=20.1 min, 1,3-dimethyl-uracil ; Peak 5 : RT=21.2 min, 1,3-dimethyl-thymine; Peak 6: RT=25.4 min, N,N,9-trimethyl-adenine; peak 7,9: RT=27.4 and 28.6 min, 1,7-dimethyl-hypoxanthine; peak 8: RT=28.1 min, N,N,3-trimethyl-adenine; peak 10: RT=30.0 min, 2'-deoxy-3-methyl-3',5'-di-O-methyl-Uridine; peak 11: RT=30.44 min, 2'-deoxy-N,O,O-trimethyl-thymidine ; peak 12 : RT=33.0 min, 2'-deoxy-N,O,O,O- tetramethyl-Adenosine.

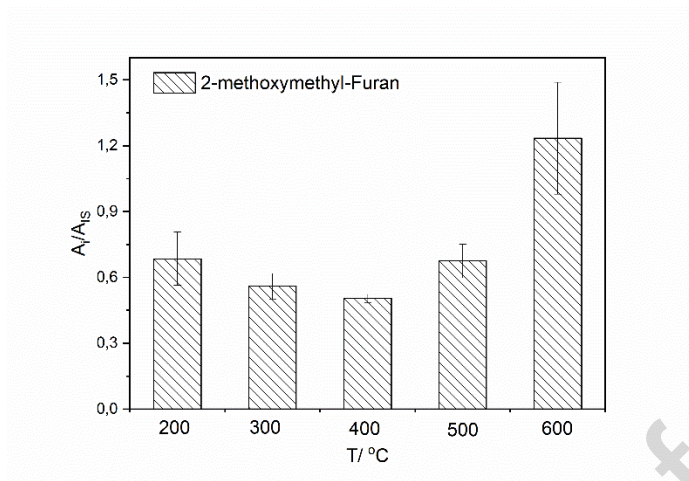


Figure 7 Abundance of methyl furfuryl detected after TMAH thermochemolysis of nucleosides at different temperatures ( $A_i/A_{IS}$  is the ratio of the chromatographic peak area of 2-methoxymethyl-furan and the chromatographic peak area of the internal standard).

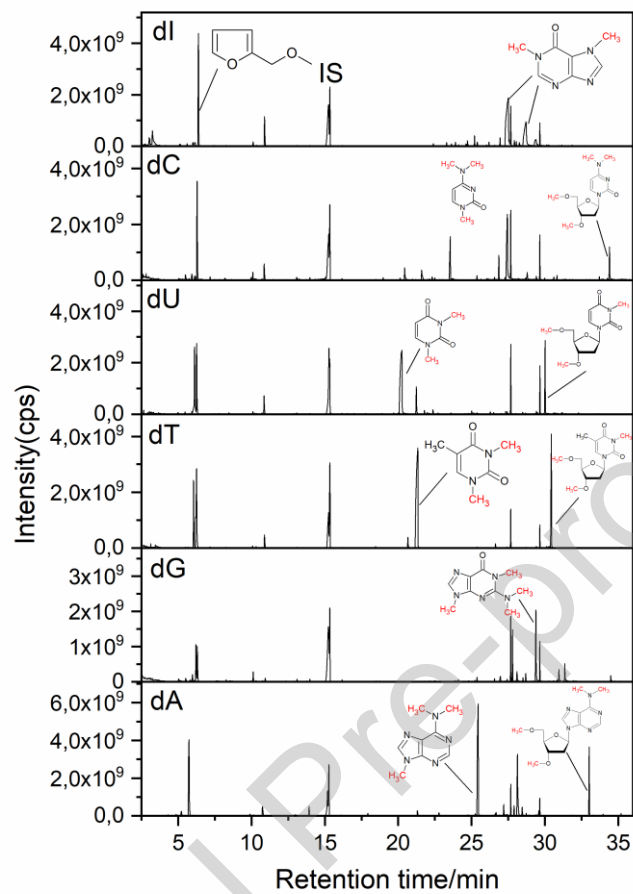


Figure 8 Chromatograms of the products of TMAH thermochemolysis of nucleosides under a SAM-like ramp pyrolysis. The signal plotted is the total ion current of the MS detector. IS stands for internal standard (Naphthalene-D8).

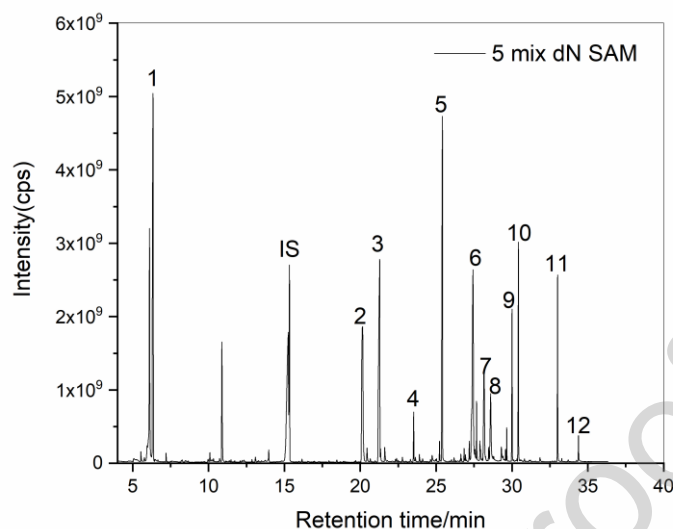


Figure 9 The chromatogram following a SAM-like ramp pyrolysis of the mixture of nucleosides. Peak 1: Furfuryl methyl ether; 2: 1,3-dimethyl-uracil; 3: 1,3-dimethyl-thymine; 4: trimethyl-cytosine; 5: N,N,9-Trimethyl-adenine; 6,8: 1,7-dimethyl-hypoxanthine; 7: N,N,3-Trimethyl-adenine; 9: 2'-Deoxy-3-methyl-3',5'-di-O-methyl-Uridine; 10: 2'-Deoxy-3-methyl-3',5'-di-O-methyl-Thymidine; 11: 2'-deoxy-N,N,O,O-tetramethyl-adenosine; 12: 2'-deoxy-N,N,O,O-tetramethyl-cytidine. IS stands for internal standard (Naphthalene-D8).

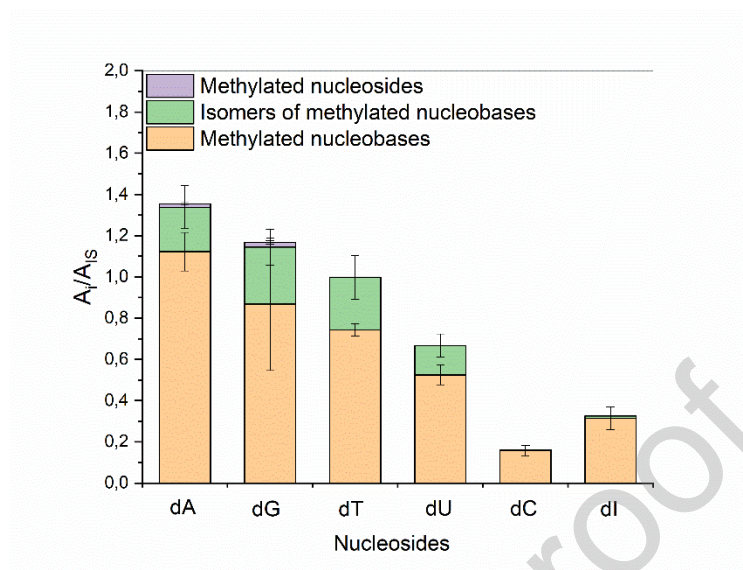


Figure 10 The abundance of each methylated nucleoside detected by Py-GC/MS under a SAM-like ramp pyrolysis with TMAH thermochemolysis.

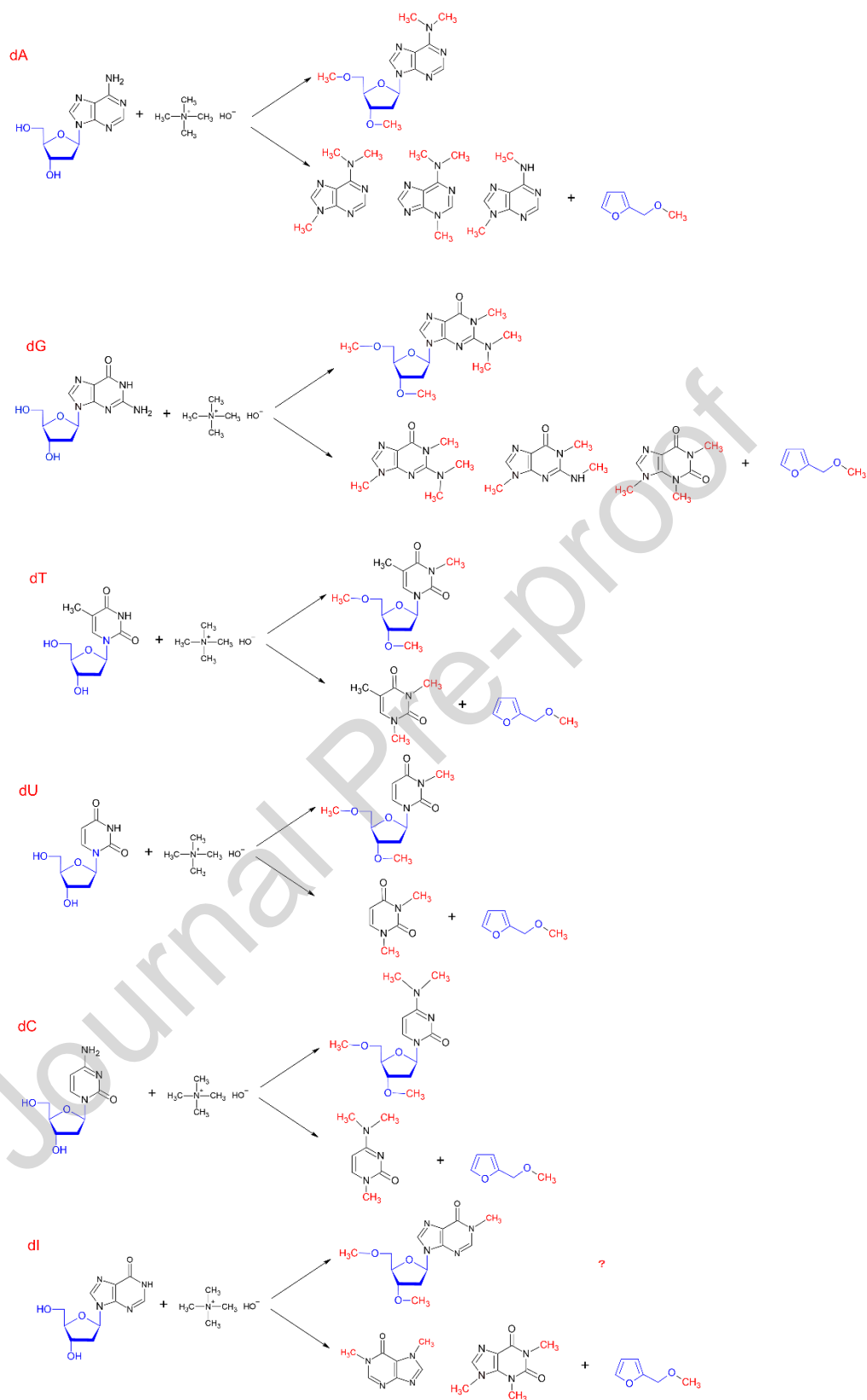


Figure 11 The TMAH thermochemolysis schemes of six nucleosides.

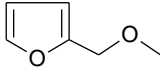
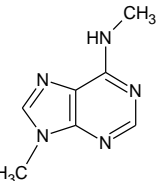
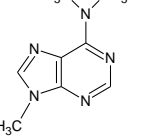
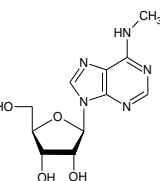
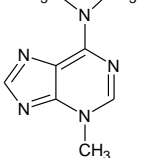
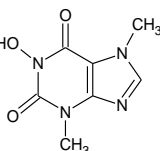
Table 1 Detailed information of nucleoside samples and solutions used in this study.

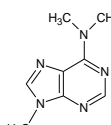
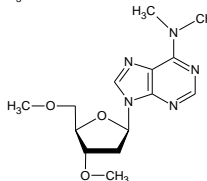
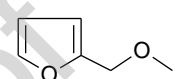
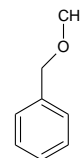
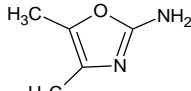
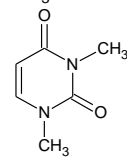
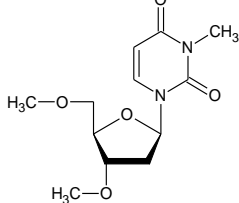
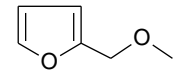
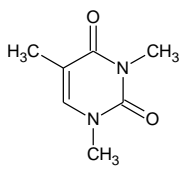
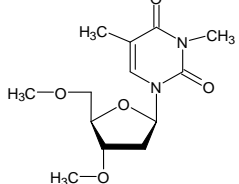
Compounds	Molecular Weight (g·mol <sup>-1</sup> )	Amount (nmol)	Injection volume (μl)	Concentration (mol·L <sup>-1</sup> )
-----------	---	---------------	-----------------------	--------------------------------------



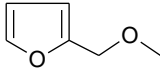
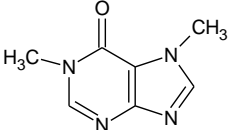
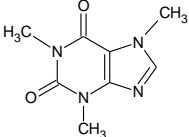
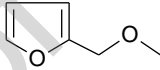
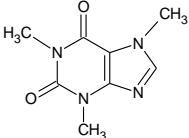
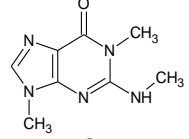
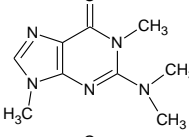
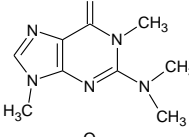
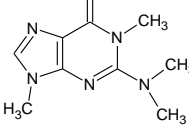
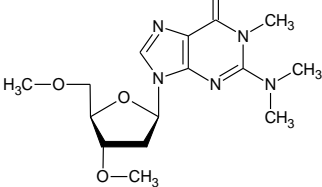
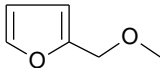
dA		269	25	0.5	0.05
dG		285	10	1.0	0.01
dT		242	25	0.5	0.05
dU		228	25	0.5	0.05
dC		227	25	0.5	0.05
dI		252	25	0.5	0.05
Mixtures	dA	269	2	0.2	0.01
	dT	242	2	0.2	0.01
	dU	228	2	0.2	0.01
	dC	227	2	0.2	0.01
	dI	252	2	0.2	0.01

Table 2 The products of nucleosides and nucleotides with TMAH thermochemolysis at 200 °C

	RT / min	Masses of fragments* m/z	Empirical formula	Compound	Compound Structure
dA	6.10	81,112,53,97	C <sub>6</sub> H <sub>8</sub> O <sub>2</sub>	2-methoxymethyl-furan	
	25.0	163,107,135,148,80,42,53	C <sub>7</sub> H <sub>9</sub> N <sub>5</sub>	N,9-dimethyl-9H-Purin-6-amine or N,9-dimethyl-adenine	
	25.5	148,162,177,107,133,80,42,52	C <sub>8</sub> H <sub>11</sub> N <sub>5</sub>	N,N,9-Trimethyl-9H-purin-6-amine or N,N,9-Trimethyl-adenine and isomers	
	26.7	178,192,207,149,135,109,80,67,44	C <sub>11</sub> H <sub>15</sub> N <sub>5</sub> O <sub>4</sub>	N-methyl-adenosine	
	26.8	134,162,177,148,121,93,42,58	C <sub>8</sub> H <sub>11</sub> N <sub>5</sub>	N,N,3-trimethyl-3H-purin-6-amine or N,N,3-trimethyl-adenine	
	26.9	194,109,67,55,82,162,177,148,121,133	C <sub>8</sub> H <sub>10</sub> N <sub>4</sub> O <sub>2</sub>	Caffeine or 3,7-dihydro-1,3,7-trimethyl-1H-	

				purine-2,6-dione	
27.	177,135,162,120,108,42,79	$C_7H_7N_5O$	9	Trimethyl-adenine	
33.	134,163,148,192,292,307,120	$C_{14}H_{21}N_5O_3$	1	2'-deoxy-N,N,O,O-tetramethyl-adenosine and isomers	
d					
U					
6.1	81,112,53,97	$C_6H_8O_2$		2-methoxymethyl-furan and isomers	
10.	91;121;77;65;105	$C_8H_{10}O$	3	Methoxymethyl-benzene	
10.	111,45,81,99,71,53	$C_5H_8N_2O$	9	4,5-dimethyl-2-oxazolamine	
20.	140,83,42,55,111	$C_6H_8N_2O_2$	2	1,3-dimethyl-uracil	
30.	145,113,87,59,45,127,270	$C_{12}H_{18}N_2O_5$	0	2'-Deoxy-3-methyl-3',5'-di-O-methyl-uridine and isomers	
d					
T					
6.0	81,112,53,97	$C_6H_8O_2$		2-methoxymethyl-furan and isomers	
21.	154,68,97,42,140	$C_7H_{10}N_2O$	5	1,3-Dimethyl-thymidine	
30.	145,113,87,59,45,127, 284	$C_{12}H_{18}N_2O_5$	5	2'-Deoxy-3-methyl-3',5'-di-O-methyl-thymidine and isomers	

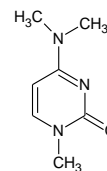
dI

6.1	81,112,53,97	$C_6H_8O_2$	2-methoxymethyl-furan	
27.5	164,107,134,81,67,53,42	$C_7H_8N_4O$	1,7-Dimethyl-hypoxanthine and isomers	
27.0	194,109,55,67,82,137,165,42	$C_8H_{10}N_4O$ 2	Caffeine	
<hr/>				
d G				
6.0	81,112,53,97	$C_6H_8O_2$	2-methoxymethyl-furan and isomers	
27.0	194,109,55,67,82,137,165,42	$C_8H_{10}N_4O$ 2	Caffeine	
27.8	207,178,192,163,149,133,121,107,42,67	$C_8H_{11}N_5O$	Trimethyl-guanine	
29.4	164,207,123,136,178,192,67,108	$C_8H_{11}N_5O$	Tetramethyl-guanine 1 and isomers	
31.0	178,109,164,67,82,55,207,192,137	$C_9H_{13}N_5O$	Tetramethyl-guanine 2 and isomers	
31.4	207,163,136,123,94,192,67,178	$C_9H_{13}N_5O$	Tetramethyl-guanine 3 and isomers	
34.5	193,164,178,150,45,59,87,337	$C_{15}H_{22}N_5O_4$	Methyl guanosine and isomers	
<hr/>				
d C				
6.1	81,112,53,97	$C_6H_8O_2$	2-methoxymethyl-Furan	

27. 153,124,138,109,82,95,42,55  
4

$C_7H_{11}N_3O$

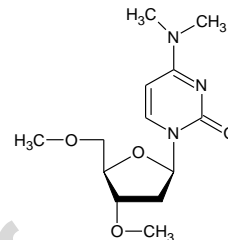
4-  
Dimethylamin  
o-1-methyl-  
2(1H)-  
pyrimidinone  
and isomers



34. 110,140,124, 153,181,45,268,252,  
4 268

$C_{13}H_{20}N_2$   
 $O_5$

2'-deoxy-  
N,N,O,O-  
tetramethyl-  
Cytidine



Journal Pre-proof

**CRedit authorship contribution statement**

**Yuanyuan He:** Conceptualization, Formal analysis, Investigation, Methodology, Writing - original draft. **Arnaud Buch:** Conceptualization, Methodology, Formal analysis, Supervision. **Cyril Szopa:** Conceptualization, Methodology, Formal analysis, Supervision. **Caroline Freissinet:** Conceptualization, Methodology, Formal analysis, Supervision. **Amy Williams:** Conceptualization, review & editing. **Melissa Guzman:** Conceptualization, review & editing. **Maëva Millan:** Conceptualization, review & editing. **David Coscia:** Conceptualization, review & editing. **Jean-Yves Bonnet:** Conceptualization, review & editing. **Michel Cabane:** Conceptualization, review & editing.

**Declaration of interests**

The authors declare that they have no known competing financial interests or personal relationships that could have appeared to influence the work reported in this paper.

**Highlights**

- Six nucleosides were analyzed under conditions relevant to Mars' instrument.
- The methylated nucleosides were detected first under SAM-like ramp pyrolysis.
- The TMAH thermochemolysis byproducts of six nucleosides were determined.
- No interaction was found among the nucleoside mixtures.
- 200 °C is the optimal thermochemolysis temperature for nucleosides and 600 °C for nucleobases.